Validation of separate multi-atlases for auto segmentation of cardiac substructures in CT-scans acquired in deep inspiration breath hold and free breathing

Spoor, Daan S.; Sijtsema, Nanna M.; van den Bogaard, Veerle A. B.; van der Schaaf, Arjen; Brouwer, Charlotte L.; Ta, Bastiaan D. P.; Vliegenthart, Rozemarijn; Kierkels, Roel G. J.; Langendijk, Johannes A.; Maduro, John H.

Published in:
Radiotherapy and Oncology

DOI:
10.1016/j.radonc.2021.07.025

Publication date:
2021

Radiotherapy and Oncology 163 (2021) 46–54

Contents lists available at ScienceDirect

Radiotherapy and Oncology

journal homepage: www.thegreenjournal.com

Original Article

Validation of separate multi-atlases for auto segmentation of cardiac substructures in CT-scans acquired in deep inspiration breath hold and free breathing

Daan S. Spoor [a], Nanna M. Sijtsema [a,*], Veerle A.B. van den Bogaard [a], Arjen van der Schaaf [a], Charlotte L. Brouwer [a], Bastiaan D.P. Ta [a], Rozemarijn Vliegenthart [b], Roel G.J. Kierkels [a], Johannes A. Langendijk [a], John H. Maduro [a], Femke B.J. Peters [a], Anne P.G. Crijns [a]

[a] Department of Radiation Oncology; and [b] Department of Radiology, University of Groningen, University Medical Center Groningen, The Netherlands

ARTICLE INFO

Article history:
Received 22 March 2021
Received in revised form 23 July 2021
Accepted 24 July 2021
Available online 31 July 2021

Keywords:
Breast cancer
Cardiac contouring
Multi-atlas based automatic segmentation
Deep inspiration breath hold

ABSTRACT

Background and purpose: Developing NTCP-models for cardiac complications after breast cancer (BC) radiotherapy requires cardiac dose-volume parameters for many patients. These can be obtained by using multi-atlas based automatic segmentation (MABAS) of cardiac structures in planning CT scans. We investigated the relevance of separate multi-atlases for deep inspiration breath hold (DIBH) and free breathing (FB) CT scans.

Materials and methods: BC patients scanned in DIBH (n = 10) and in FB (n = 20) were selected to create separate multi-atlases consisting of expert panel delineations of the whole heart, atria and ventricles. The accuracy of atlas-generated contours was validated with expert delineations in independent datasets (n = 10 for DIBH and FB) and reported as Dice coefficients, contour distances and dose-volume differences in relation to interobserver variability of manual contours. Dependency of MABAS contouring accuracy on breathing technique was assessed by validation of a FB atlas in DIBH patients and vice versa (cross-validation).

Results: For all structures the FB and DIBH atlases resulted in Dice coefficients with their respective reference contours $\geq$ 0.8 and average contour distances $\leq$ 2 mm smaller than slice thickness of (CTs). No significant differences were found for dose-volume parameters in volumes receiving relevant dose levels (WH, LV and RV). Accuracy of the DIBH atlas was at least similar to, and for the ventricles better than, the interobserver variation in manual delineation. Cross-validation between breathing techniques showed a reduced MABAS performance.

Conclusion: Multi-atlas accuracy was at least similar to interobserver delineation variation. Separate atlases for scans made in DIBH and FB could benefit atlas performance because accuracy depends on breathing technique.

Radiotherapy (RT) for both early and locally advanced breast cancer improves local and locoregional control and survival [1]. However, incidental radiation exposure to the heart increases the risk of ischemic heart disease (IHD) [2–4]. Darby et al. found that the rate of acute coronary events (ACE) increased proportionally with the mean dose to the heart (7.4% per Gy) [5], which was confirmed by a cohort study by van den Bogaard et al. [6]. These studies emphasize the need to reduce the dose received by the heart. For most left-sided breast cancer (BC) patients this can be achieved by the use of deep-inspiration breath hold (DIBH), which separates the heart from the breast during irradiation [7,8].

The relationship between cardiac dose and toxicity has been described by Normal Tissue Complication Probability (NTCP) models with the planned mean heart dose (MHD) as a prognostic variable [5,6]. Treatment factors like laterality, fractionation and DIBH result in different radiation exposure patterns for cardiac substructures, such as the atria and ventricles, which may result in different toxic events [9]. Therefore, investigating the dose to cardiac

Abbreviations: ACE, acute coronary event; DIBH, deep-inspiration breath hold; DSC, Dice similarity coefficient; FB, free breathing; LA, left atrium; LV, left ventricle; MABAS, multi-atlas based automatic segmentation; MHD, mean heart dose; NTCP, normal tissue complication probability; RA, right atrium; RV, right ventricle; V_{5Gy}, volume of left ventricle receiving 5 Gy or more; WH, whole heart.

* Corresponding author at: Department of Radiation Oncology, University Medical Center Groningen, P.O. Box 30001, 9700 RB Groningen, The Netherlands.
E-mail address: n.m.sijtsema@umcg.nl (N.M. Sijtsema).

https://doi.org/10.1016/j.radonc.2021.07.025
0167-8140/

substructuresmay be relevant to improve current NTCP-models. For example, van den Bogaard et al [6] and Spoor et al [10] showed that the LV-V_{5Gy} may be a better predictor for ACE after breast cancer radiotherapy than the MHD.

Cardiac dose-volume parameters can be obtained after the contouring of cardiac substructures. Manual contouring is time consuming and prone to interobserver variability, which may result in variation in individual dose-volume parameters, even when delineation guidelines are used [11,12]. An alternative method is multi-atlas based automatic segmentation (MABAS), which is an efficient and accurate method to generate dose-volume parameters of the heart and its substructures in breast cancer patients [13–15]. It is faster than manual contouring, even if manual corrections are required [16,17].

The ability of MABAS to deal with anatomical variation is optimal when the atlases are a representative sample of the population [18]. Because the heart is a flexible structure, its shape can be changed by the intrathoracic pressure that accompanies respiration in deep inspiration breath hold [19]. Therefore, the breathing technique used for the planning scan can affect MABAS performance.

The aim of this study was to investigate the relevance of using separate multi-atlases for automatic contouring of the whole heart, atria and ventricles in breast cancer patients treated in DIBH or free breathing (FB). Geometric and dosimetric variations caused by MABAS inaccuracies were compared to interobserver variability of manual contours.

Material and methods

Patient selection and treatment data

Fig. 1 provides an overview of the method used in the current study to generate and validate DIBH and FB atlases. In total, planning CT scans of 50 breast cancer patients were selected for this study (i.e. 20 DIBH scans and 30 FB scans). Scans were either used for atlas generation (atlas group) or atlas validation (validation group).

Jung et al. [20] showed that the performance of their multi-atlas (based on contrast-enhanced FB scanned patients) for contouring of cardiac structures plateaued for libraries containing more than 10 atlases. First, an FB multi-atlas with consensus contours of 10 patients from the FB atlas group (i.e. FB10) was created. To compensate for the absence of contrast-enhancement in our study cohort, we also created a second FB atlas by adding 10 extra patients from the FB atlas group (FB20) to include more anatomical variation. Anticipating less inter-patient anatomical variation resulting from the intrathoracic pressure that accompanies respiration only a DIBH multi-atlas with 10 consensus contour sets from the DIBH atlas group (i.e. DIBH10) was created. For both categories (i.e. DIBH and FB) 10 CT scans were selected for validation purposes.

Only planning CT scans of patients without clinically relevant anatomical abnormalities were selected. All patients were treated at the University Medical Center Groningen with 3D conformal RT using CT-based planning, as described elsewhere [21].

DIBH patients included in this study were treated in 2013 and 2014. We selected FB patients treated between 2005 and 2008, before the introduction of DIBH in our clinic. The quality of the scans and reference delineations between both datasets is comparable. Additional information on both patient cohorts can be found in Table 1 in the supplementary materials.

CT examinations were performed on a Siemens Somatom Sensation Open (Siemens Medical, Erlangen, Germany), without iodine contrast agent, slice thickness of 3 or 5 mm, field of view of 500 mm and image size of 512 × 512 pixels per slice. The scanned region extended from the tragus to 5 cm below the contralateral breast. DIBH scans were made using the Active Breathing Coordinator (ELEKTA Active Breathing Coordinator™ device, Crawley, UK) to guarantee reproducible breath volumes for every breath hold. The breath volumes were set at 70% of the maximum inspiration volumes and CT scans were acquired in a supine position on a breast board (C-Qual™ breast board, CIVCO, IOWA).

Atlas generation

Manual delineations were based on the atlas by Feng et al. [11] and included the whole heart (WH), left and right ventricle (LV, RV) and the left and right atrium (LA, RA). All manual delineations were performed in Mirada RTx (v1.6 Mirada Medical Ltd., Oxford, UK).

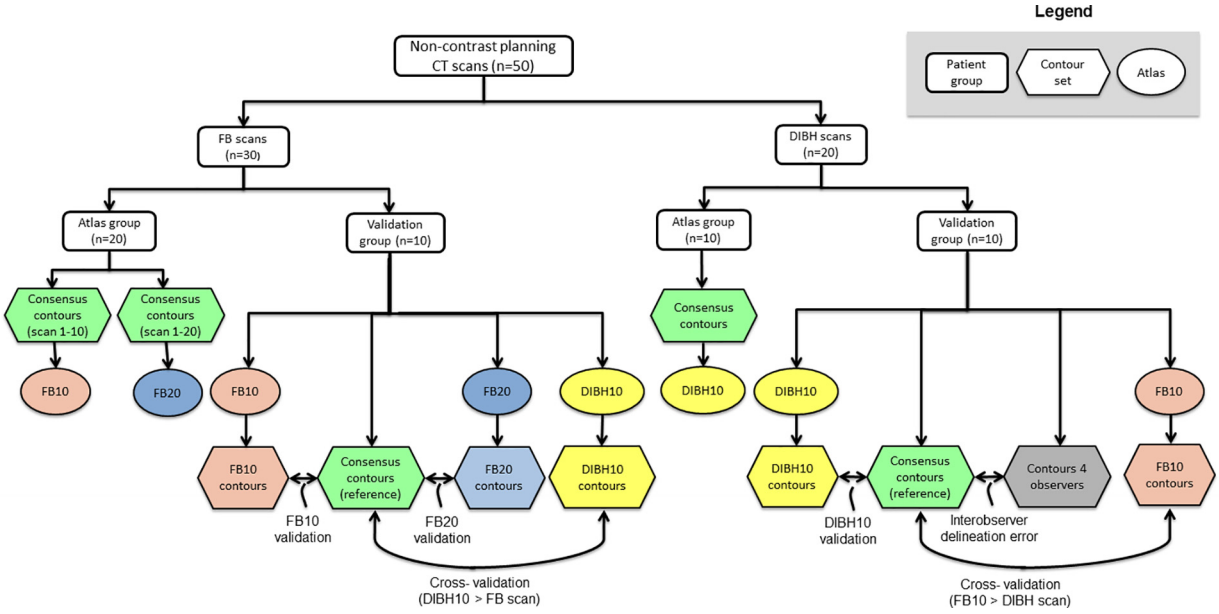

Fig. 1. Flowchart of atlas generation and (cross-)validation. Colours are used to distinguish between different (sources of) contouring sets. Abbreviations: FB = free breathing, DIBH = deep inspiration breath hold.

Multi-atlases were generated by including consensus contours of patients in the atlas group into atlas files. Multi-atlases were generated using the Mirada Workflow Box (v2.0), which used a multi-atlas segmentation approach [22].

A robust optical flow-based registration algorithm automatically aligned each of the supplied atlases to the patient case. Registration was initialized by a rigid 6 degrees of freedom registration algorithm and a mutual information based criterion was maximized (using a greedy iterative hill climbing optimization technique) when solving for the rigid transformation. Using the resulting deformation field each of the contours was mapped onto the patient image. A consensus of the contours from each atlas was found using a proprietary form of majority voting which works to sub-voxel precision.

All CT scans were delineated with the common agreement of an expert panel consisting of an experienced cardiac radiologist (RV) and a breast cancer dedicated physician assistant (FP) to create consensus contours.

Atlas validation

Atlases were validated by comparing atlas-generated contours to reference contours (because a golden standard is lacking, consensus contours were used as references) for patients in the validation group. To evaluate the impact of atlas expansion on atlas performance, the results of FB10 and FB20 validation will both be presented.

The interobserver variation in manual contouring was assessed in the DIBH validation group from a comparison of the contours from four independent observers with the reference contours. This observer group consisted of two radiation oncologists (JM, AC), a radiation oncologist resident (BT) and a breast cancer dedicated researcher (HP).

Finally, cross-validation was performed to investigate the dependency of MABAS performance on the breathing technique used in multi-atlas libraries (i.e. FB or DIBH). DIBH10 was used to generate contours in the FB validation group and FB10 generated contours in the DIBH validation group. To obtain a fair analysis of the impact of breathing technique we used the atlases based on contour sets of 10 patients (i.e. DIBH10 and FB10). Atlas-generated contours were compared to the reference contours in the corresponding validation group.

Evaluation of atlas accuracy

Atlas performance was evaluated by comparing atlas and reference contours in the validation groups. Interobserver delineation errors were evaluated by averaging the comparison between individual observers and the reference contours. Performance was evaluated by following metrics:

1) Clinical usefulness evaluated by four independent observers. Observers were unaware of the contour source (DIBH10 or another observer) and rated contours as ‘no editing required’, ‘minor editing required’ or ‘major editing required and not useful in clinical practice’ according to Hardcastle et al. [23].
2) Geometry.
   a) Dice similarity coefficients (DSC) [24]. Index for spatial overlap ranging between 0 (no overlap) and 1 (complete overlap). For all cardiac structures (i.e. whole heart, atria and ventricles), we aimed at a minimal Dice Similarity Coefficient between atlas-generated contours and reference contours of 0.8.
   b) ComGrad distances [25], which finds corresponding points between two contours by traversing a vector field based on the combined gradient of the distance transforms. Evaluations were done with an in-house developed implementation of the ComGrad method in Matlab (Version 2018a) as described by van der Put et al [25]. Average and absolute ComGrad distances were analysed.
   c) Volumes of matching contours.
3) Dosimetry. Comparison of relevant dose-volume parameters (D_{mean}, D_2, D_{98}, V_{1Gy}, V_{5Gy}) resulting from different contour sets (calculated with an in-house developed tool using the clinical 3D dose distribution and contours of cardiac substructures).
4) NTCP. Comparison of individual ACE risks for the FB validation group (clinical parameters of the DIBH validation group were incomplete) based on cardiac dose parameters resulting from MABAS or reference contours ACE risks in the first 9 years after radiotherapy were calculated using the model of van den Bogaard et al. [6], ($LV - V_{5Gy}$ as a predictor), and the model of Darby et al. [5], ($WH - D_{mean}$ as predictor). Variables used for this analysis can be found in Supplementary Materials Table 2.

Significance was assessed by non-parametric Wilcoxon signed rank tests performed in SPSS version 23.0. Spearman’s rank-order correlations were used to assess the relationship between predicted ACE risks resulting from dose parameters based on different contouring methods.

Results

Despite a difference in treatment periods for FB and DIBH scanned patients, no relevant differences in the quality of the scans and reference delineations were observed. The MABAS algorithm generated contours for the major cardiac structures (WH, RV, RA, LV, LA) in all cases. MABAS contours were generated within 5 min per patient compared to 70 min (range: 60–80 min) for manual contouring by the observers. According to the observers, 41.0% of the DIBH10 generated contours did not require editing, 54.5% required minor editing and 4.5% major editing. 48.5% of the manual delineations made by the observers were scored as ‘no editing required’, also 48.5% as ‘minor editing required’ and 3.0% as ‘major editing required’. Fig. 2 shows an example of good alignment between DIBH10-generated contours and reference contours for a DIBH CT- scan. A visual inspection of most common atlas delineation errors for the whole heart, occurring near the apex or at the anterior region, is illustrated in Supplementary material Fig. 1

Fig. 3 shows the geometric evaluation of different contouring sets. Comparison of DIBH10 generated contours with their reference contours resulted in DSCs > 0.8 for all (Fig. 3B). Validation of FB10 resulted in a DSC < 0.8 for the LA and RV, but for FB20 the DSCs were >0.8 for all structures (Fig. 3A).

Atlas-generated contours were of equal size, or smaller (LA, LV and RV for FB20; RV for DIBH10), than reference contours (Supplementary material Fig. 2). The average distance between surfaces of FB20 or DIBH10 contours towards their respective reference contours was $\leq$2 mm for all structures (Fig. 3C and D), while on average the absolute distance between atlas and reference contours was $\leq$4 mm or less (Fig. 3E and F).

Observer contours of the ventricles were less consistent with reference contours than the DIBH10 contours expressed by a reduced DSC and increased absolute ComGrad distances (Fig. 3B and F). For all structures, average ComGrad distances to the reference contours were < 2 mm and similar for DIBH10 contours and observer contours (Fig. 3D).

Fig. 4 shows results of the cross-validation. In general, the performance of FB10 on DIBH scans as well as DIBH10 on FB scans was

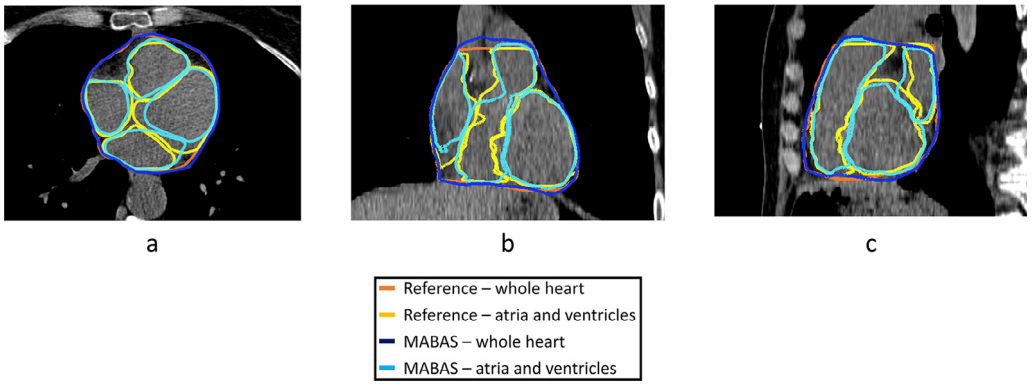

Fig. 2. Different views (a: transversal, b: coronal, c: sagittal) of the agreement of MABAS (DIBH10) generated contours and reference contours for a DIBH CT- scan. Abbreviations: MABAS = multi-atlas based automatic segmentation.

worse than the application of atlases created with the breathing method corresponding to the scans (Fig. 4).

The impact of the contouring method on the resulting cardiac dose-volume parameters was limited. Differences in dose parameters were only seen in the RA for DIBH10 contours and in the LA for observer contours with respect to the reference contours (Fig. 5). Supplementary Fig. 3 shows similar results for the FB validation set where differences were only found in the LA and the FB20 did not result in more accurate dose-volume parameters than the FB10. Supplementary Figs. 4 and 5 also present the results per treatment side, but differences were not statistically evaluated given the limited sample sizes (i.e. 5 patients per treatment side).

No differences were observed between NTCP-values for ACE risks calculated with the Darby model using FB10 atlas contours and those based on FB reference contours (p = 0.594). Similarly, no differences were found for NTCP-values calculated with the van den Bogaard model (p = 0.465). As shown in Fig. 6, a Spearman's rank-order correlation test showed a strong and positive correlation between ACE risks calculated with dose parameters based on FB10 contours versus reference contours (ρ = 1.000, p < 0.01 in both prediction models).

Discussion

Our study showed that separate atlases for DIBH and FB scanned BC patients are reliable and efficient tools for the contouring of cardiac substructures and calculating cardiac dose parameters or NTCP-values. The clinical usefulness of both DIBH10 generated contours and manual contours was similar. Using a multi-atlas library consisting of consensus contours from 10 DIBH patients resulted in good spatial overlap (DSC $\geq$ 0.8) with reference contours in all structures (i.e. heart, atria and ventricles). Such agreement was also achieved for the FB atlas including 20 FB scanned patients. Local differences between atlas and reference contours, quantified by average and absolute ComGrad distances, were comparable to the pixel size of the CT scans. The accuracy of DIBH10 was at least similar to, and for the ventricles better than, the interobserver variation in manual delineation. Cross-validation showed reduced MABAS performance when a FB atlas was applied to CT-scans acquired in DIBH and vice versa. No differences were found for dose-volume parameters in the volumes receiving relevant dose levels (WH, LV and RV), and no differences were found in NTCP-values based on dose parameters obtained from atlas or reference contours.

Further improvement of atlas accuracy might be achieved by integration of an iterative atlas selection procedure or a genetic selection strategy to identify the best subset of atlases within the multi-atlas library [26,27]. Atlas generated contours can also be improved by correcting large errors [16,17]. Based on the results of our study it would be advisable to perform a quick visual check focusing on regions identified in Supplementary Materials Fig. 1. Delineation errors near the apex of the heart are likely related to low image contrast between the apex and the surrounding structures such as the diaphragm, liver and the bifurcation of the pulmonary arteries. Furthermore, these structures show relatively large variations in shape and position between patients, thereby complicating atlas-based segmentation. Another region of common MABAS errors is the pericardial tissue (found on the anterior surface of the heart [28]) which shows little image contrast with surrounding tissue. Delineation errors in this area, which receives the highest dose in breast cancer RT, could potentially affect the dose-volume parameters. However, the atria were the only regions where significant differences between dose parameters obtained from MABAS or reference contours were found (see Fig. 5). In breast cancer radiotherapy, the atria receive a relative low dose (average D_2, <3 Gy) and therefore these differences are less important for development of NTCP models for cardiac toxicity.

DIBH10 generated contours of the ventricles had a higher spatial overlap with reference contours (made by the expert panel) compared to contours made by group of four independent observers. The ventricular septum has little contrast on planning scans and apparently MABAS, based on consensus contours created by an expert panel with great knowledge of the anatomy of the heart, was more consistent in delineating the ventricular septum than independent observers.

In general, expanding a multi-atlas library results in better performance, although the optimal size depends on methods used [29]. The optimal number of scans per atlas was not evaluated because current performances already met our clinical goal. However, DSCs > 0.8 for all structures were only found for the FB atlas consisting of 20 patients while for the DIBH atlas this goal was met with 10 patients included. As mentioned earlier, the heart is flexible and its shape can be changed by the intrathoracic pressure that accompany respiration in deep inspiration breath hold [19]. Most likely, the respiratory motion during FB scans increased anatomical variations of the heart, thereby affecting MABAS performance when insufficient patients are included. It was also shown that applying FB10 to DIBH scanned patients and vice versa reduced MABAS performance. Increased intrathoracic pressure associated with DIBH may result in systematically different anatomical variation in the heart and MABAS performance would be affected when this specific variation is not represented in the multi-atlas library. This suggests that ideally separate atlases are used for auto-contouring of cardiac structures in FB and DIBH scanned patients.

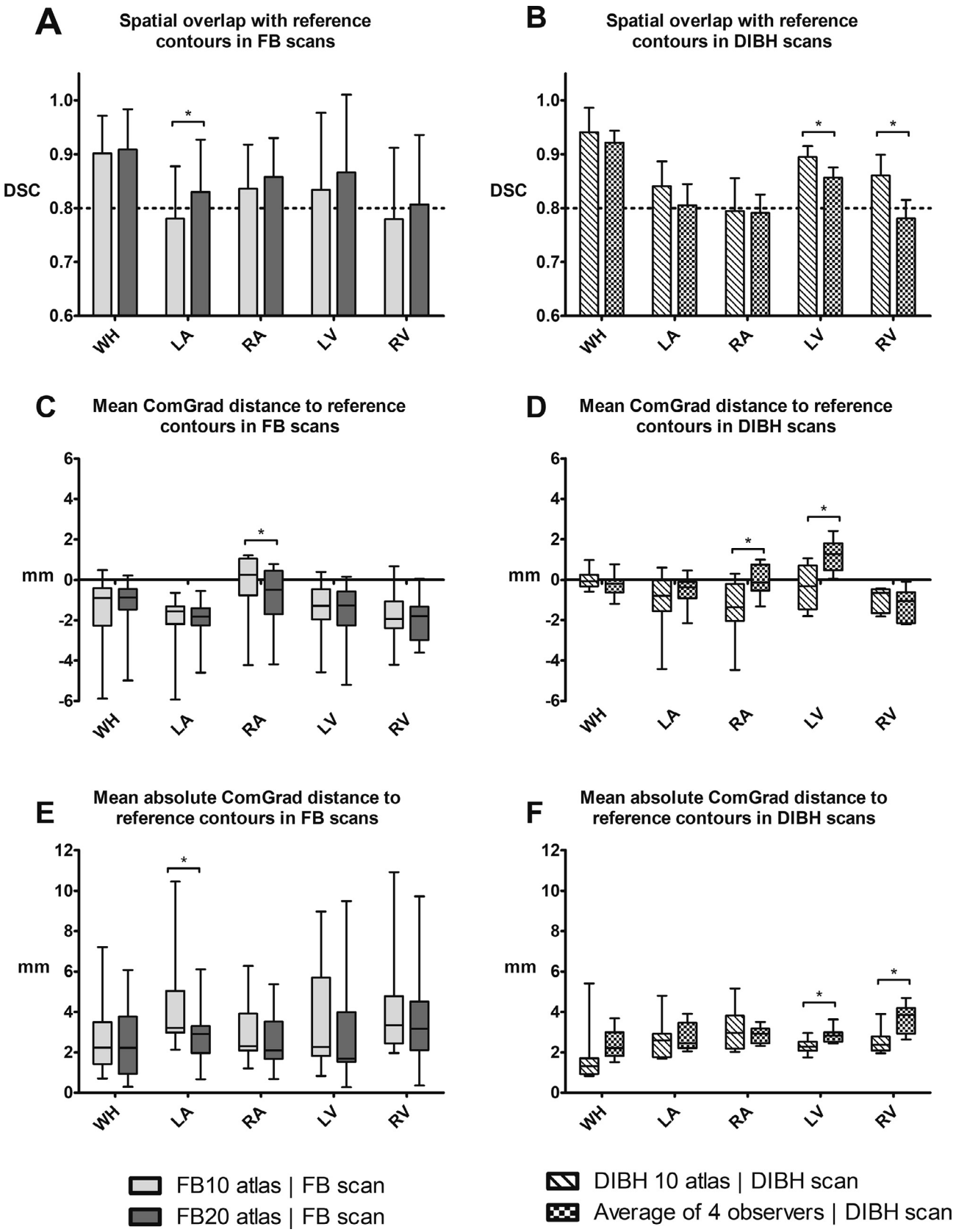

Fig. 3. Geometric validation of contouring methods. Statistically significant differences are highlighted with an asterisk (Wilcoxon signed rank test, $p < 0.05$). Abbreviations: DSC = dice similarity coefficient, FB = free breathing, DIBH = deep inspiration breath hold, WH = whole heart, LA = left atrium, RA = right atrium, LV = left ventricle and RV = right ventricle.

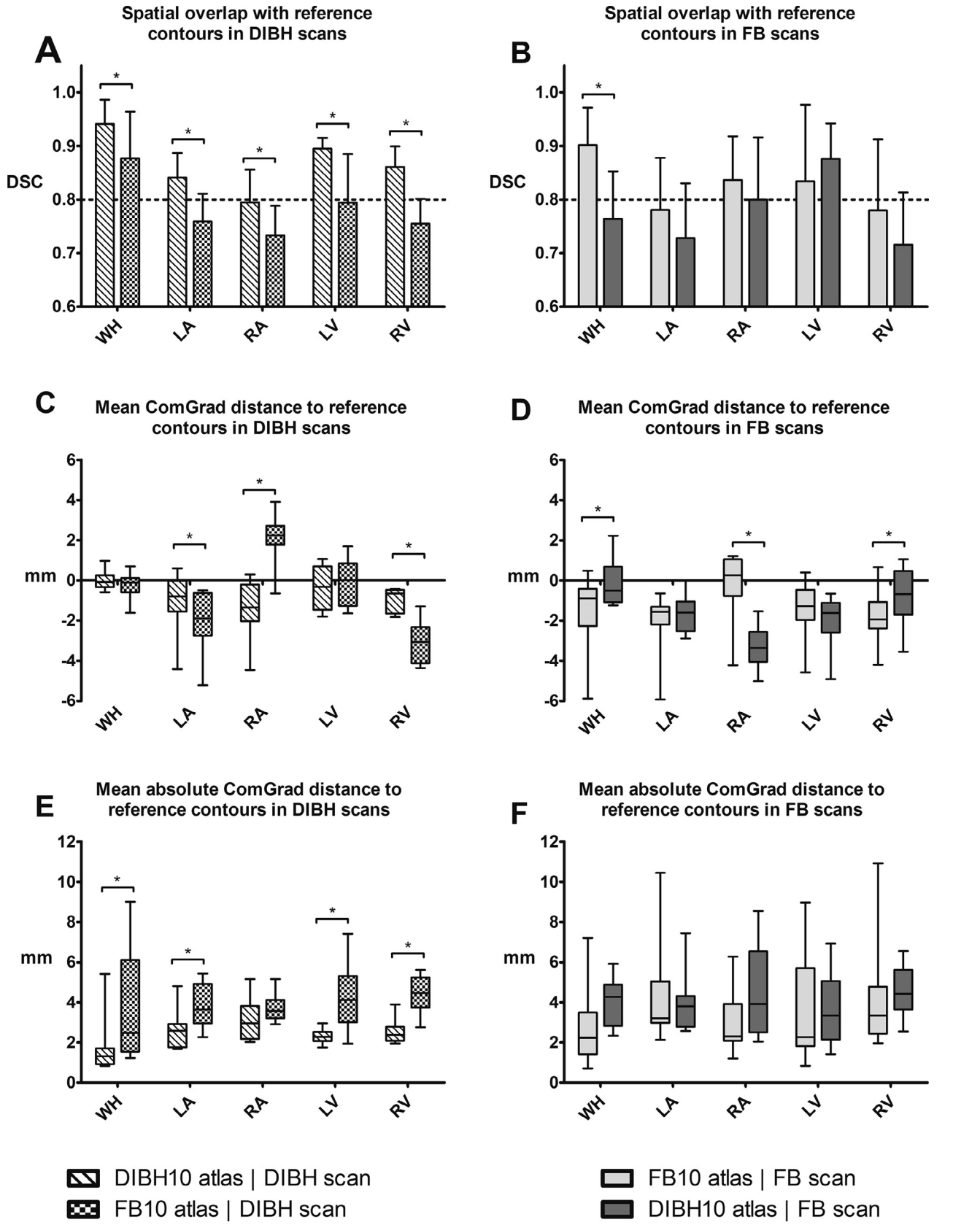

Fig. 4. Geometric cross-validation of different contouring methods. Statistically significant differences are highlighted with an asterisk (Wilcoxon signed rank test, $p < 0.05$). Abbreviations: DSC = dice similarity coefficient, FB = free breathing, DIBH = deep inspiration breath hold, WH = whole heart, LA = left atrium, RA = right atrium, LV = left ventricle and RV = right ventricle.

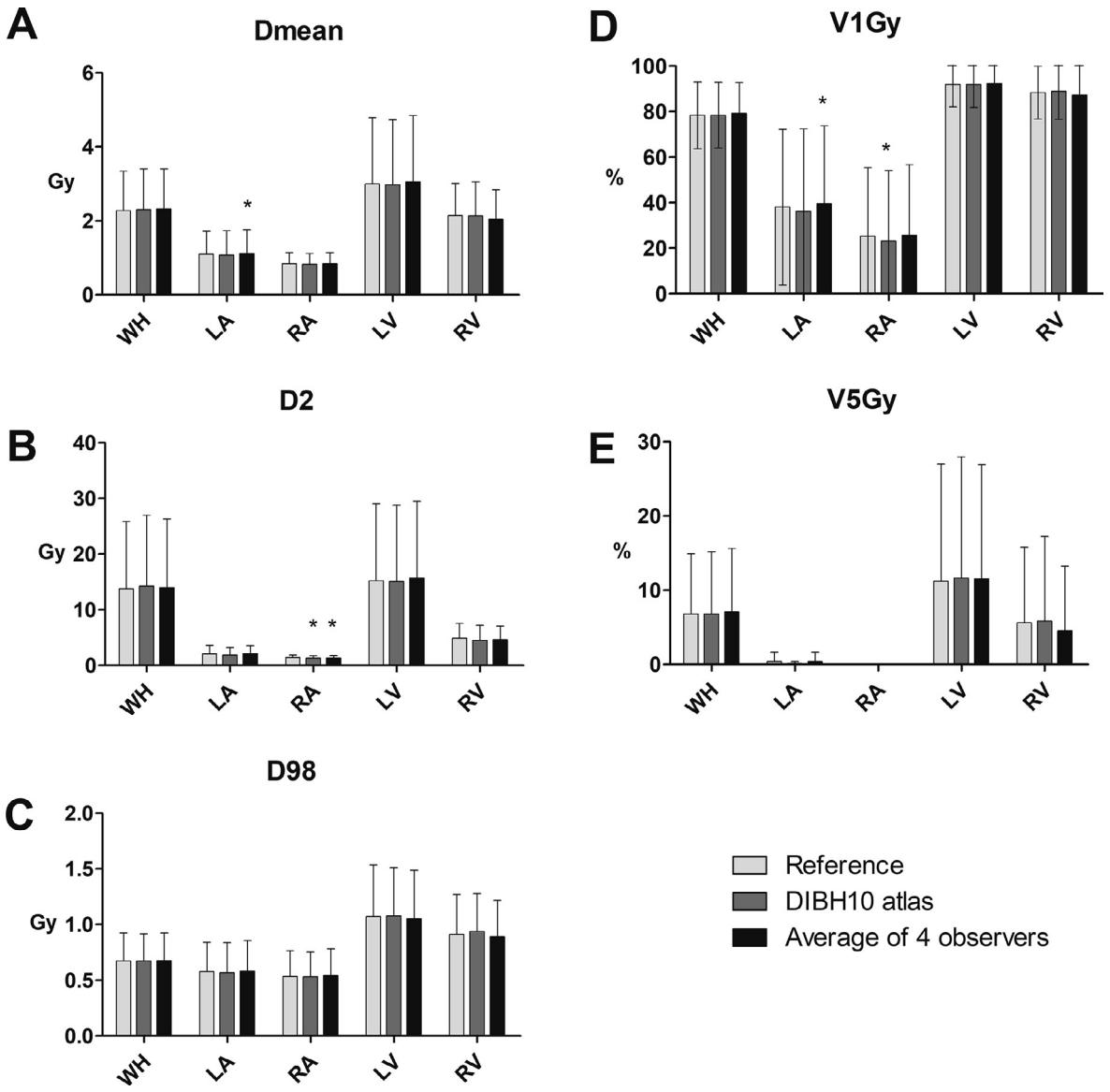

Fig. 5. Dose parameters in major cardiac structures obtained from different contouring methods applied to DIBH planning scans ($n = 10$). Statistically significant differences of dose parameters relative to reference contours are highlighted with an asterisk (Wilcoxon signed rank test, $p < 0.05$). Abbreviations, FB = free breathing, DIBH = deep inspiration breath hold, WH = whole heart, LA = left atrium, RA = right atrium, LV = left ventricle and RV = right ventricle.

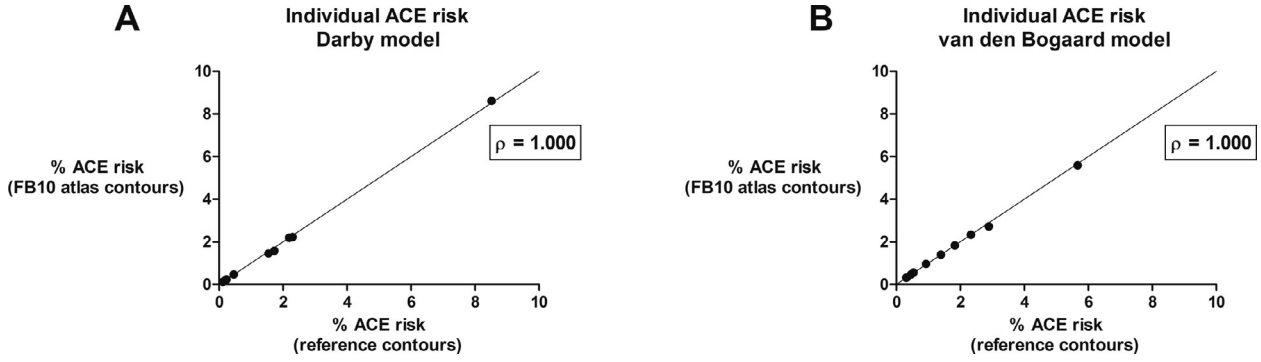

Fig. 6. Effect of contouring method (FB10 atlas vs. reference) on the individual ACE risk in 10 FB planned patients. Abbreviations: ACE = acute coronary event, FB = free breathing.

In general, the results of the current study are in line with other studies that investigated atlas based auto-segmentation for contouring of the heart on CT scans [13–17,20,30–33]. Loap et al. [22] were able to create an atlas with better accuracy for the whole heart although delineations of the atria and ventricles were less accurate. Kaderka et al [14] found similar performances compared to our study but did not create separate atlases for FB and DIBH and atlas accuracy was not compared to the interobserver delineation errors.

As an extension to MABAS, the paper by Finnegan et al [34] describes a method for automatic delineation of cardiac structures which incorporates inter-observer variation in contour generation. Anonther alternative to MABAS is deep learning [35,36]. We briefly investigated an algorithm combining the Maastro DLC model for the WH [36] and an in-house developed algorithm in Mirada RTx for the atria and ventricles (training set with 109 contours sets made with MABAS followed by manual corrections). However, larger and more consistent training sets were required to possibly reach accuracies similar to our multi-atlases.

The usability of our multi-atlases could be improved by allowing contouring of other cardiac areas like coronary arteries, cardiac valves or conduction system structures [37]. Initially, the goal of this study was to include coronary arteries in the MABAS but they were only generated in 4% of the cases and were therefore left out from further analysis. An alternative to contouring of the left anterior descending (LAD) artery, which receives the highest dose of all coronaries, is contouring of a high-risk cardiac zone [38]. Hence, we developed and validated an alternative auto-segmentation tool for the LAD based on anatomical landmarks obtained from contours of the ventricles [39]. In future studies, the multi-atlases developed in the current study, together with this LAD tool, can be used to calculate cardiac dose-volume parameters on a large scale for the development of NTCP models for cardiac toxicities.

Conclusion

This study showed that MABAS performance depends on the breathing technique used in planning scans. To optimize atlas performance, separate atlases for DIBH and FB scanned patients can be used to include the most representative anatomical variation within the multi-atlas library. Atlases developed and validated in this study are reliable and efficient tools for contouring of cardiac substructures and obtaining cardiac dose parameters with accuracies at least similar to interobserver delineation variation.

Conflict of interest

None.

Appendix A. Supplementary data

Supplementary data to this article can be found online at https://doi.org/10.1016/j.radonc.2021.07.025.

References

[1] Early Breast Cancer Trialists' Collaborative Group (EBCTCG). Effect of radiotherapy after breast-conserving surgery on 10-year recurrence and 15-year breast cancer death: meta-analysis of individual patient data for 10 801 women in 17 randomised trials. Lancet 2011;378:1707–16. https://doi.org/10.1016/S0140-6736(11)61629-2.

[2] Harris EER, Correa C, Hwang W-T, Liao J, Litt HI, Ferrari VA, et al. Late cardiac mortality and morbidity in early-stage breast cancer patients after breast-conservation treatment. J Clin Oncol 2006;24:4100–6. https://doi.org/10.1200/JCO.2005.05.1037.

[3] Nilsson G, Holmberg L, Garmo H, Duvernoy O, Sjögren I, Lagerqvist B, et al. Distribution of coronary artery stenosis after radiation for breast cancer. J Clin Oncol 2012;30:380–6. https://doi.org/10.1200/JCO.2011.34.5900.

[4] Correa CR, Litt HI, Hwang W-T, Ferrari VA, Solin LJ, Harris EE. Coronary artery findings after left-sided compared with right-sided radiation treatment for early-stage breast cancer. J Clin Oncol 2007;25:3031–7. https://doi.org/10.1200/JCO.2006.08.6595.

[5] Darby SC, Ewertz M, McGale P, Bennet AM, Blom-Goldman U, Brønnum D, et al. Risk of ischemic heart disease in women after radiotherapy for breast cancer. N Engl J Med 2013;368:987–98. https://doi.org/10.1056/NEJMoa1209825.

[6] van den Bogaard VAB, Ta BDP, van der Schaaf A, Bouma AB, Middag AMH, Bantema-Joppe EJ, et al. Validation and modification of a prediction model for acute cardiac events in patients with breast cancer treated with radiotherapy based on three-dimensional dose distributions to cardiac substructures. J Clin Oncol 2017;35:1171–8. https://doi.org/10.1200/JCO.2016.69.8480.

[7] Remouchamps VM, Letts N, Vicini FA, Sharpe MB, Kestin LL, Chen PY, et al. Initial clinical experience with moderate deep-inspiration breath hold using an active breathing control device in the treatment of patients with left-sided breast cancer using external beam radiation therapy. Int J Radiat Oncol Biol Phys 2003;56:704–15. https://doi.org/10.1016/S0360-3016(03)00010-5.

[8] McIntosh A, Shoushtari AN, Benedict SH, Read PW, Wijesooriya K. Quantifying the reproducibility of heart position during treatment and corresponding delivered heart dose in voluntary deep inhalation breath hold for left breast cancer patients treated with external beam radiotherapy. Int J Radiat Oncol Biol Phys 2011;81:e569–76. https://doi.org/10.1016/j.ijrobp.2011.01.044.

[9] Loap P, Kirova Y. Evaluating cardiac substructure radiation exposure in breast rotational intensity modulated radiation therapy: effects of cancer laterality, fractionation and deep inspiration breath-hold. Cancer/Radiotherapie 2021;25:13–20. https://doi.org/10.1016/j.canrad.2020.05.016.

[10] Spoor D, Leeuwen FEV, Russell N, Boekel NB, Jacob S, Combs SE, et al. Development and internal validation of an NTCP-model for acute coronary events after breast cancer radiotherapy: first results of the MEDIRAD BRACE study (H2020-Euratom-1.4 / 755523). Int J Radiat Oncol 2020;108:S11–2. https://doi.org/10.1016/j.ijrobp.2020.07.2088.

[11] Feng M, Moran JM, Koelling T, Chughtai A, Chan JL, Freedman L, et al. Development and validation of a heart atlas to study cardiac exposure to radiation following treatment for breast cancer. Int J Radiat Oncol Biol Phys 2011;79:10–8. https://doi.org/10.1016/j.ijrobp.2009.10.058.

[12] Lorenzen EL, Taylor CW, Maraldo M, Nielsen MH, Offersen BV, Andersen MR, et al. Inter-observer variation in delineation of the heart and left anterior descending coronary artery in radiotherapy for breast cancer: a multi-centre study from Denmark and the UK. Radiother Oncol 2013;108:254–8. https://doi.org/10.1016/j.radonc.2013.06.025.

[13] Lorenzen EL, Ewertz M, Brink C. Automatic segmentation of the heart in radiotherapy for breast cancer. Acta Oncol (Madr) 2014;53:1366–72. https://doi.org/10.3109/0284186X.2014.930170.

[14] Kaderka R, Gillespie EF, Mundt RC, Bryant AK, Sanudo-Thomas CB, Harrison AL, et al. Geometric and dosimetric evaluation of atlas based auto-segmentation of cardiac structures in breast cancer patients. Radiother Oncol 2019;131:215–20. https://doi.org/10.1016/j.radonc.2018.07.013.

[15] Zhou R, Liao Z, Pan T, Milgrom SA, Pinnix CC, Shi A, et al. Cardiac atlas development and validation for automatic segmentation of cardiac substructures. Radiother Oncol 2017;122:66–71. https://doi.org/10.1016/j.radonc.2016.11.016.

[16] Eldesoky AR, Yates ES, Nyeng TB, Thomsen MS, Nielsen HM, Poortmans P, et al. Internal and external validation of an ESTRO delineation guideline – dependent automated segmentation tool for loco-regional radiation therapy of early breast cancer. Radiother Oncol 2016;121:424–30. https://doi.org/10.1016/j.radonc.2016.09.005.

[17] Stross WC, Herchko SM, Vallow LA. Atlas based segmentation in prone breast cancer radiation therapy. Med Dosim 2020;45:298–301. https://doi.org/10.1016/j.meddos.2020.02.004.

[18] Iglesias JE, Sabuncu MR. Multi-atlas segmentation of biomedical images: a survey. Med Image Anal 2015;24:205–19. https://doi.org/10.1016/j.media.2015.06.012.

[19] Jagsi R, Moran JM, Kessler ML, Marsh RB, Balter JM, Pierce LJ. Respiratory motion of the heart and positional reproducibility under active breathing control. Int J Radiat Oncol Biol Phys 2007;68:253–8. https://doi.org/10.1016/j.ijrobp.2006.12.058.

[20] Jung JW, Lee C, Mosher EG, Mille MM, Yeom YS, Jones EC, et al. Automatic segmentation of cardiac structures for breast cancer radiotherapy. Phys Imaging Radiat Oncol 2019;12:44–8. https://doi.org/10.1016/j.phro.2019.11.007.

[21] Van der Laan HP, Dolsma WV, Maduro JH, Korevaar EW, Langendijk JA. Dosimetric consequences of the shift towards computed tomography guided target definition and planning for breast conserving radiotherapy. Radiat Oncol 2008;3:1–8. https://doi.org/10.1186/1748-717X-3-6.

[22] Loap P, Tkatchenko N, Kirova Y. Evaluation of a delineation software for cardiac atlas-based autosegmentation: an example of the use of artificial intelligence in modern radiotherapy. Cancer/Radiotherapie 2020;24:826–33. https://doi.org/10.1016/j.canrad.2020.04.012.

[23] Hardcastle N, Tomé WA, Cannon DM, Brouwer CL, Wittendorp PWH, Dogan N, et al. A multi-institution evaluation of deformable image registration algorithms for automatic organ delineation in adaptive head and neck radiotherapy. Radiat Oncol 2012;7. https://doi.org/10.1186/1748-717X-7-90.

[24] Dice LR. Measures of the amount of ecologic association between species. Ecology 1945;26:297–302. https://doi.org/10.2307/1932409.

[25] van der Put RW, Raaymakers BW, Kerkhof EM, van Vulpen M, Lagendijk JJW. A novel method for comparing 3D target volume delineations in radiotherapy.

Phys Med Biol 2008;53:2149–59. https://doi.org/10.1088/0031-9155/53/8/010.
[26] Finnegan R, Lorenzen E, Dowling J, Holloway L, Thwaites D, Brink C. Localised delineation uncertainty for iterative atlas selection in automatic cardiac segmentation. Phys Med Biol 2020;65:035011. https://doi.org/10.1088/1361-6560/ab652a.
[27] Antonelli M, Cardoso MJ, Johnston EW, Appayya MB, Presles B, Modat M, et al. GAS: A genetic atlas selection strategy in multi-atlas segmentation framework. Med Image Anal 2019;52:97–108. https://doi.org/10.1016/j.media.2018.11.007.
[28] Groban L, Garner CR. TEE Pocket Manual. Chapter 15: Pericardial Disease. TEE Pocket Man., 2018, p. 224. 10.1016/B978-0-323-52280-9.00015-X.
[29] Schipaanboord B, Boukerroui D, Peressutti D, van Soest J, Lustberg T, Kadir T, et al. Can atlas-based auto-segmentation ever be perfect? Insights from extreme value theory. IEEE Trans Med Imaging 2019;38:99–106. https://doi.org/10.1109/TMI.2018.2856464.
[30] Duane F, Aznar MC, Bartlett F, Cutter DJ, Darby SC, Jagsi R, et al. A cardiac contouring atlas for radiotherapy. Radiother Oncol 2017;122:416–22. https://doi.org/10.1016/j.radonc.2017.01.008.
[31] Arsène-Henry A, Xu HP, Robilliard M, El Amine W, Costa KYM. Evaluation of an automatic delineation system for organs at risk and target lymph nodes volumes for patients treated for breast cancer. Cancer/Radiotherapie 2018;22:241–7. https://doi.org/10.1016/j.canrad.2017.09.012.
[32] Ciardo D, Gerardi MA, Vigorito S, Morra A, Dell'acqua V, Diaz FJ, et al. Atlas-based segmentation in breast cancer radiotherapy: evaluation of specific and generic-purpose atlases. Breast 2017;32:44–52. https://doi.org/10.1016/j.breast.2016.12.010.
[33] Mitchell RA, Wai P, Colgan R, Kirby AM, Donovan EM. Improving the efficiency of breast radiotherapy treatment planning using a semi-automated approach. J Appl Clin Med Phys 2017;18:18–24. https://doi.org/10.1002/acm2.12006.
[34] Finnegan R, Dowling J, Koh E-S, Tang S, Otton J, Delaney G, et al. Feasibility of multi-atlas cardiac segmentation from thoracic planning CT in a probabilistic framework. Phys Med Biol 2019;64:085006. https://doi.org/10.1088/1361-6560/ab0ea6.
[35] Yang J, Veeraraghavan H, Armato SG, Farahani K, Kirby JS, Kalpathy-Kramer J, et al. Autosegmentation for thoracic radiation treatment planning: a grand challenge at AAPM 2017. Med Phys 2018;45:4568–81. https://doi.org/10.1002/mp.13141.
[36] Lustberg T, van Soest J, Gooding M, Peressutti D, Aljabar P, van der Stoep J, et al. Clinical evaluation of atlas and deep learning based automatic contouring for lung cancer. Radiother Oncol 2018;126:312–7. https://doi.org/10.1016/j.radonc.2017.11.012.
[37] Loap P, Servois V, Dhonneur G, Kirov K, Fourquet A, Kirova Y. A radiation therapy contouring atlas for cardiac conduction node delineation. Pract Radiat Oncol 2021;11:e434–7. https://doi.org/10.1016/j.prro.2021.02.002.
[38] Loap P, Tkatchenko N, Nicolas E, Fourquet A, Kirova Y. Optimization and auto-segmentation of a high risk cardiac zone for heart sparing in breast cancer radiotherapy. Radiother Oncol 2020;153:146–54. https://doi.org/10.1016/j.radonc.2020.09.044.
[39] van den Bogaard VAB, van Dijk LV, Vliegenthart R, Sijtsema NM, Langendijk JA, Maduro JH, et al. Development and evaluation of an auto-segmentation tool for the left anterior descending coronary artery of breast cancer patients based on anatomical landmarks. Radiother Oncol 2019;136:15–20. https://doi.org/10.1016/j.radonc.2019.03.013.